GEOGRAPHICAL ANALYSIS

ORIGINAL ARTICLE

Assessment of Population Displacement Dynamics Influencing Urban Heat Risk Using the Geospatial Analysis During the Syrian Crisis in Latakia City

Suzan Karmoka[1*], **Ashok D Hanjagi**[1]

1 *Department of Geography and GeoInformatics, Bangalore University, Jnana Bharathi, Bengaluru, 560056, Karnataka, India.*

OPEN ACCESS

Received: 05.02.2025
Accepted: 25.10.2025
Published: 22.12.2025

Citation: Karmoka S, Hanjagi AD. Assessment of Population Displacement Dynamics Influencing Urban Heat Risk Using the Geospatial Analysis During the Syrian Crisis in Latakia City. 2025; 14(2):53-61. https://doi.org/10.53989/bu.ga.v14i2.25.27

* **Corresponding author.**
karmoka.suzan@hotmail.com

Funding: None

Competing Interests: None

Published By Bangalore University, Bengaluru, Karnataka

ISSN
Print: 2319-5371
Electronic: xxxx-xxxx

Abstract

Many developing countries face challenges in urban planning, often failing to allocate sufficient space, particularly green areas, to support healthy living conditions and essential services. Latakia, Syria, exemplifies this issue, especially following the massive influx of displaced populations due to the Syrian crisis over the past decade. As one of the country's safest cities, Latakia has experienced significant population pressure, leading to unregulated urban expansion at the expense of green spaces. This unplanned growth has intensified the urban heat island (UHI) effect. To assess the rising UHI effect in Latakia, this study applied the Heat Risk Index (HRI), calculated using a five-degree weighting system. The findings indicate that in 2013, no sector exhibited extreme heat risk, with levels ranging from mild to severe. However, by 2023, heat risk had escalated across most sectors. Notably, Al Sleibeh and Al-Raml Aljanobi sectors reached extreme heat risk levels, correlating with population increases of 64% and 24%, respectively. Meanwhile, the Southern Corniche and Mashrou Alqalaa sectors maintained moderate risk levels. The Al-Datour sector demonstrated the most significant change, with its HRI rising by two levels to a severe risk category, primarily due to an 8% urban expansion over agricultural lands. To mitigate UHI effects, Latakia urgently requires innovative adaptation strategies. Addressing climate change impacts and population pressures necessitates strategic, localized planning. HRI can serve as a foundation for these efforts by pinpointing priority areas for targeted adaptation interventions.

Keywords: Heat Risk Index, Latakia, Population Density, Urban Heat Islands

1 Introduction

Urban Heat Island (UHI) refers to the phenomenon in which metropolitan regions experience significantly higher temperatures than their surrounding rural areas. This effect is primarily driven by human activities that alter the natural properties of the land surface and atmosphere. As cities grow and expand, they replace natural land cover with impermeable surfaces such as asphalt, concrete, and buildings. These materials absorb and retain heat, leading to elevated temperatures. The significant modifications in land use and land cover contribute to the formation of the UHI effect [1]. Assessing land cover changes provides valuable insights into the impact of human activities on the ecological conditions of urban environments [2].

Urbanization and rapid population growth are among the leading causes of the degradation and loss of natural vegetation and arable land [3]. Developing countries, in particular, exhibit pronounced land use and land cover transformations resulting from extensive human activities [4]. Researchers worldwide have observed considerable urban expansion associated with thermal variations and ecological disturbances in rapidly growing cities. Urbanization influences the microclimate by altering local land surface temperatures, increasing energy consumption, and contributing to greenhouse gas emissions [5, 6].

Several studies have highlighted the growing importance of understanding urban heat islands and their impacts on cities. Researchers have found that urban expansion has significantly affected major cities such as New Delhi, Mumbai, Chennai, Tokyo, Los Angeles, and Cairo. As urbanization continues to expand, more cities are likely to experience similar challenges, emphasizing the urgent need for effective mitigation strategies to address UHI and promote sustainable urban development. Many Mediterranean cities, for instance, share common characteristics of densely built settlements with limited green spaces and extensive use of impervious materials, exacerbating heat stress [7, 8]. Climate change further amplifies these challenges, making it essential to implement adaptation strategies.

In densely populated metropolitan areas with minimal vegetation, the increasing frequency of heat waves has drawn attention to the correlation between temperature rise and land use patterns. The loss of natural spaces, combined with urban layouts that disrupt wind circulation, contributes to the intensification of the UHI effect [9]. Poor urban planning is a key factor exacerbating this issue [10].

Latakia, Syria, serves as a prime example of a city struggling with unplanned urban expansion, especially following waves of population displacement caused by the Syrian crisis. As one of the country's safest cities, Latakia has experienced significant population pressure, resulting in urban sprawl at the expense of green spaces. This study assesses the impact of increasing population density and subsequent urban expansion in Latakia, particularly in relation to climate change, to propose effective mitigation and adaptation strategies.

2 Study area

The study area is located in the northwestern part of Syria [Fig. 1], within the administrative boundaries of Latakia governorate. This study covered 16 sectors. The highest population density is in the western sectors of the city, which are associated with both commercial and residential activities. The majority of the city's marketplaces and logistical infrastructure are located in these highly populated sectors. Eastern and northern sectors have business, residential, and agricultural activities [11]. Low-density informal housing was created when the rich agricultural fields were progressively urbanized.

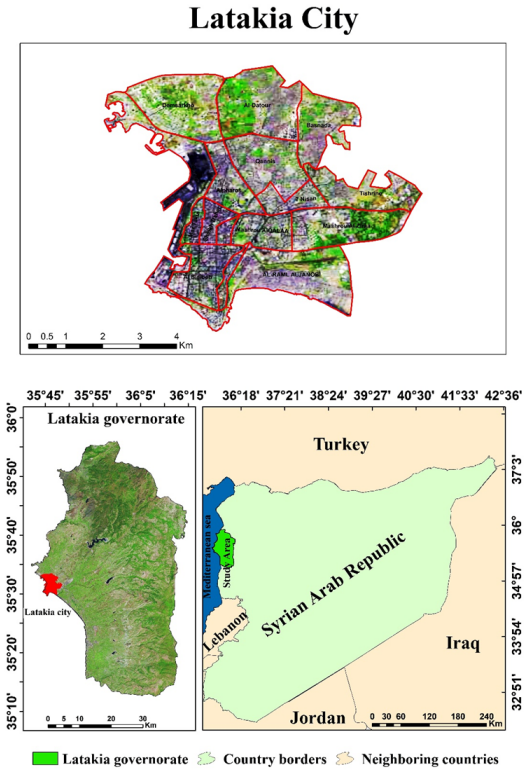

Fig. 1: Study Area map

3 Materials and methods

3.1 Materials

- 30m spatial resolution Landsat 8 image downloaded from the EOS Land Viewer website (https://eos.com/landviewer). to calculate NDVI and LST [Table. 1].

Table 1: Details of the satellite images utilized

Satellite	Sensor	Date of acquisition	Spatial resolution (m)	Cloud cover land	Path/Row
Landsat 8	OLI	04/07/2013	30	0.64	174/35
Landsat 8	OLI	16/07/2023	30	0.02	174/35

In these images, the study area remained cloud-free, as the cloud cover was concentrated in a different part of the scene.

- Map of the administrative borders of Latakia city according to the Ministry of Local Administration and Environment data.
- Due to Syria's ongoing crisis, recent population data is unavailable, with the last official census in 2011. To estimate Latakia's population, high-resolution OpenStreetMap imagery was used to count residential buildings. Assuming an average household size of five, estimates were adjusted for displacement impacts in 2023. Data was cross-referenced with UNOCHA, revealing a population increase from approximately 616,410 in 2013 to 762,370 in 2023, highlighting significant demographic shifts over the decade.

3.2 Data collection

This study was conducted in August 2013 and August 2023, representing the hottest summer months when the UHI effect is most intense in Syria. 2013 was chosen as it marks the onset of large-scale displacement to Latakia due to the Syrian crisis. A ten-year comparison assesses how this population shift impacted UHI. Landsat 8 satellite images were used to derive Land Surface Temperature (LST) and Normalized Difference Vegetation Index (NDVI), key indicators for analyzing UHI effects and human impacts on the environment [12].

3.3 Methodology

The heat risk index was calculated using 3 criteria in the ArcGIS Pro software, where the weighted sum analysis techniques are used to determine the heat risk over the study area. The population density, LST values, and non-vegetation coverage are used for heat risk identification. These criteria were used together to show the impact of population distribution dynamics on the change in urban areas and its impact on the shrinkage of green spaces in the city and the resulting increase in the effect of urban heat islands.

a) LST was calculated using the following steps:

Land Surface Temperature (LST) data plays a vital role in analyzing the impacts of climate change on both urban and rural regions. It offers a direct measure of surface temperature, enabling researchers to identify areas with notable thermal fluctuations. These variations are often influenced by factors such as population density and human activities, which significantly contribute to the UHI effect and broader surface temperature changes across different landscapes [13, 14]. To calculate the LST, the algorithm applied by [15] using ERDAS IMAGINE was adopted as follows:

1. The transformation of the digital number (DN) to spectral radiance (L) (Conversion to Top of Atmosphere (TOA) Radiance):

$L(\lambda) = ML \times Band\ 10 + AL - Oi$

Where:

- L(λ): TOA spectral radiance.
- ML: Radiance multiplicative band.
- AL: Radiance adds band.
- Oi: correction value for Band 10.

2. Conversion to Top-of-Atmosphere (TOA) Brightness Temperature, Kelvin (k) to Celsius degree C^o:

$BT = K2 / \ln(k1/L(\lambda)+1) - 273.15$

Where:

- BT: Top of Atmosphere brightness temperature Co
- L(λ): TOA spectral radiance
- *K*1 and *K*2 stand for the band-specific thermal conversion constants from the metadata.

3. Normalized Difference Vegetation Index (NDVI):

NDVI = (NIR-RED) / (NIR+RED)

4. Minimum and maximum NDVI values are used for the proportion of vegetation calculation:

$$PV = ((NDVI - NDVI\ min) / (NDVImax - NDVImin))^2$$

5. The land surface emissivity (LSE) is calculated based on the proportion of vegetation:

$$E = 0.004 * PV + 0.986$$

6. Land Surface Temperature (LST) Calculation:

$$LST = BT / (1+ (\lambda * BT / C2) * \ln (E))$$

Where:

- BT: Top of Atmosphere brightness temperature Co.
- λ: Wavelength of emitted radiance, for Landsat8 Band#10 λ= 10.8.
- E: Land Surface Emissivity.
- C2 = h*c/s C2= 14388 mK.
- h: Plank's constant = 6.626 * 10-34 J s.
- s: Boltzmann constant = 1.38*10-23 J/K.

We choose the highest temperature in each sector within the study area after driving the LST index. Consequently, the HRI first input is done.

b) Derivation of the NDVI:

The Normalized Difference Vegetation Index (NDVI) is a widely used indicator for monitoring vegetation conditions and distinguishing green vegetation from bare soil [16]. It helps assess vegetation quantity and detect changes over time [17]. Spectral vegetation indices are globally applied to evaluate vegetation health in both natural and cultivated landscapes [18-22].

After generating the NDVI map, the region was classified into vegetation and non-vegetation areas. The number of pixels in each class was calculated, and their percentage was determined. The non-vegetation percentage serves as a second input for computing the HRI.

c) Calculation of population density:

Each of the 16 sectors population densities was determined by dividing the total number of inhabitants by the neighborhood's area. Thus, the third input for RHI is done.

Because a higher population density will result in a greater demand for structures, which is linked to a reduction in the amount of green space in cities, it will be easier to show how population density exacerbates the urban heat island phenomenon, so Heat Risk Index.

d) Calculation of Heat Risk Index (HRI):

Once the input variables have been processed, they can be integrated to generate HRI [Fig. 2]. The three derived input variables for HRI should be combined into a single shapefile layer. This layer will encompass all the studied sectors, ensuring that each sector is associated with its corresponding data from the three input variables within the attribute table.

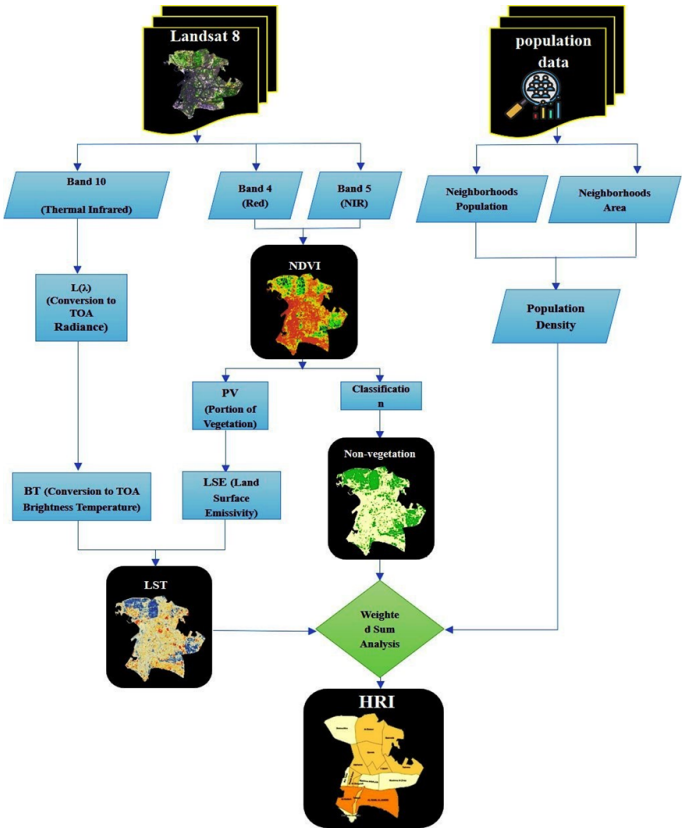

Fig. 2: Flowchart of Research Methodology

The input variables use different units of measurement and must be standardized before being combined. The Standardize Field geoprocessing tool was applied to standardize the units for the three input variables using ArcGIS Pro. The minimum-maximum standardization method is used to standardize the input variables and create a 5-point scale where 1 represents areas with the

lowest heat risk index and 5 represents areas with the highest heat risk index, as follows: No Risk, Mild, Moderate, Severe, and Extreme Risk.

The three-input criteria data were converted into raster format classified from 1 to 5, as the weighted sum tool requires raster inputs. The number 1 indicates a low value in the impact on the HRI, and the higher the number, the higher the impact, until we reach the number 5, which is the most influential class on the HRI.

4 Results and discussions

4.1 Land Surface Temperature Effects

The first input generated is LST. As observed in the maps [Fig. 3], a comparison between 2013 and 2023 reveals a slight temperature increase over the decade. This rise is attributed to recurrent drought events and a general decline in rainfall during this period [23-25].

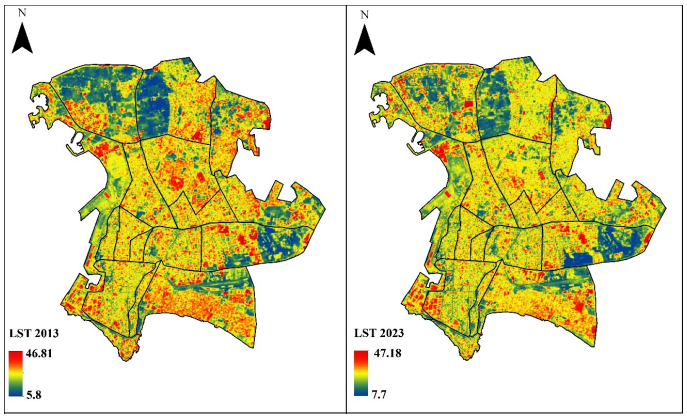

Fig. 3: Land Surface Temperature maps

In 2023, there is a noticeable reduction in low-temperature areas compared to 2013, as these regions have shifted to higher temperatures. This trend is particularly evident in the Al-Datour and Demsarkho sectors, where urban expansion and green space reduction, driven by population pressure and internal displacement, have led to rising temperatures. Similar patterns were observed in Tartous, where built-up areas nearly doubled during the crisis [26].

After classifying temperatures into five classes, Basnada, Al-Pharous, and Al-Raml Aljanobi followed class 5 (high temperatures) in 2013. By 2023, Demsarkho, Al-Datour, and Tishrine had also reached class 5, while Al-Pharous shifted to class 4 due to declining temperatures [Fig. 4].

Only a few sectors, like Mar Takla, Al Owaynah and Tabiyat, kept the same temperature class over these years and remained associated with temperature class 1, whereas the majority of sectors had temperature increases during these ten years. Land cover type, especially vegetation cover, plays a crucial role in shaping the microclimate by influencing the exchange of energy between the land and atmosphere [27] which in turn alters temperature and precipitation patterns. Urbanization and shrinking green spaces in cities are key processes that can significantly increase exacerbating global warming [5].

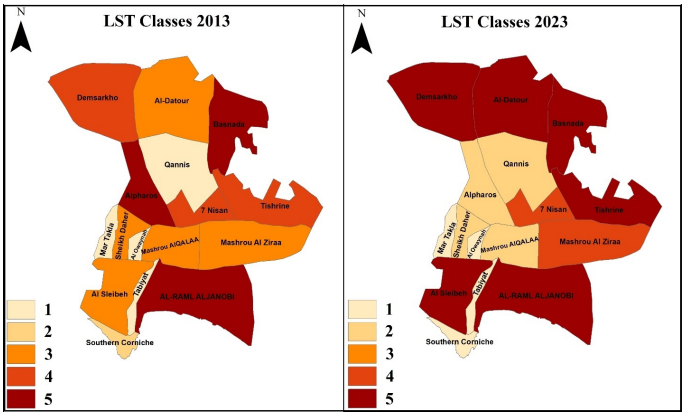

Fig. 4: Land Surface Temperature classes maps

4.2 Non-Vegetation Cover Effects

Vegetation-covered areas play a crucial role in moderating the climate in cities as they reduce warmth and increase shade. Therefore, locating vegetation-free zones within the city is a key step toward limiting the sites that contribute to increasing the severity of the HRI.

The NDVI maps for the study area were generated for the years 2013 and 2023. As observed in [Fig. 5], the majority of sectors maintained a relatively stable percentage of vegetation cover, with minimal changes in either increase or decrease. However, a noticeable decline in green areas is evident in certain northern sectors, particularly in Demsarkho and Al-Datour.

This reduction can be attributed to urban expansion, driven by the increased demand for housing due to internal displacement during the Syrian crisis. Notably, these sectors previously consisted of more than 50% agricultural land, making the loss of vegetation particularly significant. The impact extends beyond the intensification of the urban heat island effect, leading to adverse

environmental consequences for agricultural systems and economic repercussions. Furthermore, as indicated in [Table. 2], the proportion of non-vegetated land increased by approximately 4% in 2023 compared to 2013.

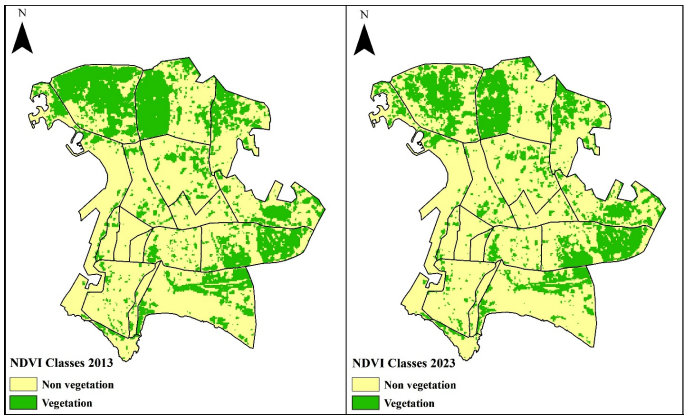

Fig. 5: Normalized Difference Vegetation Index classes maps

Table 2. Land cover area in percentage

Land cover type	2013	2023
Vegetation cover	29.5	25.4
Non vegetation cover	70.5	74.6

By classifying the NDVI map into two main categories vegetation cover and non-vegetation cover a new map was derived based on the percentage of non-vegetated areas [Fig. 6]. This map was further classified into five categories according to the proportion of vegetation cover. Class 1 represents the areas with the highest percentage of vegetation cover, while Class 5 corresponds to those with the lowest vegetation cover. Consequently, Class 5 has the most significant influence on increasing the severity of the heat risk index due to the limited presence of green spaces.

As illustrated in [Fig. 6], most sectors have experienced a decline in vegetation cover. Notably, the city center, particularly the sectors of Mar Takla, Alpharos, and Qannis, has shifted to Class 5, indicating the lowest percentage of vegetation cover. The primary factor contributing to the reduction in green spaces in these central sectors is high population density. Additionally, these sectors have a smaller spatial extent compared to others. In the case of AL-Raml Aljanobi sector, vegetation cover has also declined, placing it in Class 4. This sector has undergone significant unplanned and irregular urban expansion, largely due to the high influx of displaced persons.

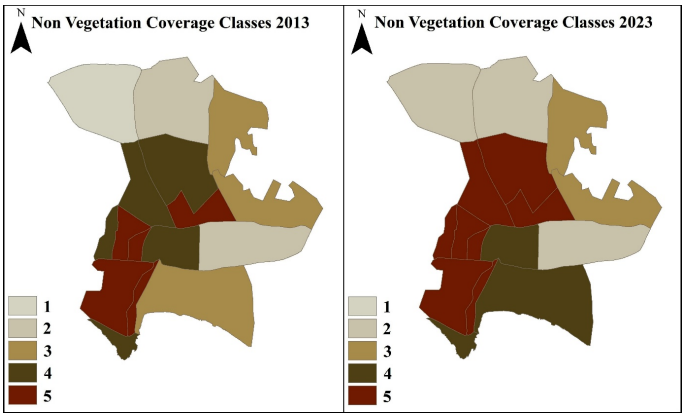

Fig. 6: Non vegetation coverage classes maps

4.3 Population Density Effects

In our case study of Latakia city, demographic changes due to internal displacement during the Syrian crisis have been the most significant factor influencing the heat risk index. A comparison of population density between 2013 and 2023 [Fig. 7] indicates that the overall population increase across all sectors was substantial; its impact on urban heat island intensity is evident. The increasing population has been observed to drive substantial urban expansion, encroaching upon forested and agricultural lands [28-31].

This is particularly due to the city's reception of a disproportionately high number of displaced persons relative to its area, whereas as of February 2022, the number of IDPs in Latakia governorate was stated to be 449,317. According to UNOCHA, as the administrative center of the governorate, Latakia absorbed the largest share of displaced individuals, resulting in significant population pressure across the city.

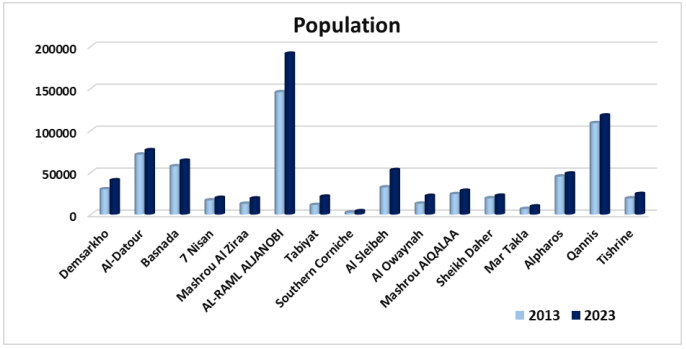

Fig. 7: Population data for the study area sectors

Notably, [Fig. 7] shows that the Al Owaynah and Tabiyat sectors, both located in the city center, experienced the most significant population growth in 2023, nearly doubling compared to 2013. In analyzing the population factor, population density was calculated and classified into five categories, similar to the previous factors. The maps [Fig. 8] illustrate the spatial distribution of these classes across the studied sectors. The highest population density was recorded in Al Owaynah, the smallest sector, which transitioned from Class 3 in 2013 to Class 5, the highest density category, in 2023. Additionally, five other sectors Mar Takla, Al Sleibeh, Tabiyat, 7 Nisan, and Al-Datour experienced an increase in population density classification over this period.

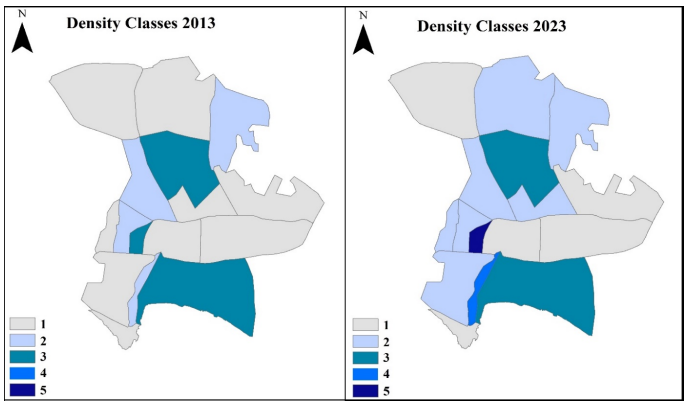

Fig. 8: Population density classes maps

Notably, the AL-Raml Aljanobi sector remained in Class 3 in both 2013 and 2023. However, despite this classification, it had the highest population among all sectors and is one of the largest in the study area. As a result, its population density did not appear high relative to its size. Nevertheless, the sector experienced significant population pressure due to the limited number of residential buildings and the presence of barren lands.

4.4 Heat Risk Index (HRI) Distribution

Using the three previously analyzed factors, a map of HRI classes was generated, [Fig. 9]. In 2013, none of the sectors fell into the extreme risk class. However, four sectors Damsarkho, Al-Datour, Mar Takla, and Mashrou Al Ziraa were classified under the Mild class. These sectors were characterized by extensive green spaces, except for Mar Takla, where vegetation cover played a crucial role in mitigating the local climate conditions.

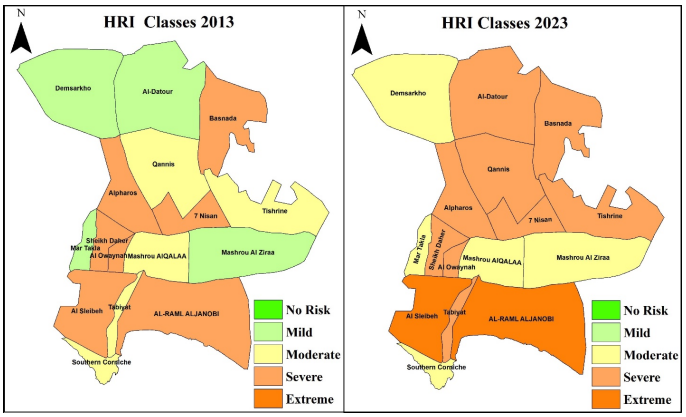

Fig. 9: Heat Risk Index classes maps

Furthermore, in 2013, none of the sectors fell into the No Risk category, indicating that all sectors were already at a critical stage. Without intervention measures to enhance green spaces and implement climate mitigation strategies, the risk of urban heat island impacts could escalate.

By 2023, most sectors saw an increase in HRI levels, with Al Sleibeh and Al-Raml Aljanobi reaching the extreme risk category due to significant population pressure. Al Sleibeh experienced 24% population growth, while Al-Raml Aljanobi's population surged by 64%, alongside a rise in buildings and a decline in green spaces [Fig. 10]. This contradicts modern urban planning research, which emphasizes large-scale tree planting as the most effective solution for mitigating urban heat stress, improving air quality, and enhancing overall environmental sustainability [10].

Fig. 10: Google Earth images illustrate how the built-up area and vegetation cover changed from 2013 to 2023 in AL-Raml Aljanobi sector

The Al-Datour sector was the only area where the HRI increased by two levels, reaching a severely dangerous category in 2023. This escalation is mainly due to an 8% increase in urban expansion, particularly over agricultural lands. As shown in [Fig. 11], extensive agricultural fields

and fruit orchards have been replaced with buildings, exacerbating heat retention.

Fig. 11: Google Earth images illustrate how the built-up area and vegetation cover changed from 2013 to 2023 in Al-Datour sector

The loss of vegetation, essential for temperature regulation, has intensified the urban heat island effect.

This sector highlights the urgent need for sustainable urban planning that balances development with green space preservation. Proposed mitigation strategies include tree-planting programs, high-albedo materials, and climate-responsive land-use planning [32-34].

The impact of effective urban planning is particularly evident in the Southern Corniche sector, which has maintained a moderate HRI classification over the past decade [Fig. 12]. This stability can be attributed to its development in accordance with urban planning standards that prioritize adequate green spaces, as well as the absence of significant building expansion during this period. Additionally, population growth in this sector was minimal, nearly negligible. It is also a sector overlooking the sea, as the proximity to the sea helps mitigate heat accumulation from concrete structures, reducing the overall urban heat effect.

Fig. 12: Google Earth images illustrate how the built-up area and vegetation cover changed from 2013 to 2023 in Southern Corniche sector

5 Conclusion

The findings revealed that in 2013, none of the sectors experienced extreme heat risk; instead, risk levels ranged from mild to severe. However, by 2023, heat risk levels increased in most sectors, with Al Sleibeh and Al-Raml Aljanobi reaching extreme heat risk due to significant population growth. Meanwhile, Southern Corniche and Mashrou Alqalaa maintained a moderate heat risk level. Notably, Al-Datour was the only sector where the HRI increased by two levels, reaching a severely dangerous category. This surge was driven by rapid urban expansion, particularly over agricultural lands.

The analysis shows that most HRI changes in urban areas are linked to rising population density or urban expansion, often at the expense of green spaces. Temperature played an indirect role, whereas direct impacts were due to internal displacement, increasing population pressure. This highlights the need for re-planning to accommodate population growth, encouraging suburban development and expanding green spaces to counterbalance the city's current deficiency.

To combat urban heat island effects, the city must adopt innovative adaptation strategies. The HRI can serve as a foundational tool to identify high-risk areas, guiding localized adaptation plans that prioritize climate resilience, sustainable urban planning, and increased green coverage.

6 Acknowledgments

The first author expresses gratitude to the Indian Council for Cultural Relations (ICCR) for providing all the available support.

References

1. Jiang J, Tian G. Analysis of the impact of Land use/Land cover change on Land Surface Temperature with Remote Sensing. *Procedia Environmental Sciences*. 2010;2:571-575.10.1016/j.proenv.2010.10.062
2. Pandey B, Joshi PK, Seto KC. Monitoring urbanization dynamics in India using DMSP/OLS night time lights and SPOT-VGT data. *International Journal of Applied Earth Observation and Geoinformation*. 2013;23:49-61.10.1016/j.jag.2012.11.005
3. Liu Y, Wang Y, Peng J, Du Y, Liu X, Li S, *et al*. Correlations between Urbanization and Vegetation Degradation across the World's Metropolises Using DMSP/OLS Nighttime Light Data. *Remote Sensing*. 2015;7(2):2067-2088.10.3390/rs70202067

4. Baker JL. Bangladesh-Dhaka: Improving Living Conditions for the Urban Poor. 2007;.10.11588/xarep.00003567
5. Santos MJ, Smith AB, Dekker SC, Eppinga MB, Leitão PJ, Moreno-Mateos D, *et al*. The role of land use and land cover change in climate change vulnerability assessments of biodiversity: a systematic review. *Landscape Ecology*. 2021;36(12):3367-3382.10.1007/s10980-021-01276-w
6. Rahaman S, Kumar P, Chen R, Meadows ME, Singh RB. Remote Sensing Assessment of the Impact of Land Use and Land Cover Change on the Environment of Barddhaman District, West Bengal, India. *Frontiers in Environmental Science*. 2020;8.10.3389/fenvs.2020.00127
7. Chorianopoulos I, Pagonis T, Koukoulas S, Drymoniti S. Planning, competitiveness and sprawl in the Mediterranean city: The case of Athens. *Cities*. 2010;27(4):249-259.10.1016/j.cities.2009.12.011
8. Chen L, Yu B, Yang F, Mayer H. Intra-urban differences of mean radiant temperature in different urban settings in Shanghai and implications for heat stress under heat waves: A GIS-based approach. *Energy and Buildings*. 2016;130:829-842.10.1016/j.enbuild.2016.09.014
9. Akbari H, Cartalis C, Kolokotsa D, Muscio A, Pisello AL, Rossi F, *et al*. Local Climate Change and Urban Heat Island Mitigation Techniques - The State of the Art. *Journal of Civil Engineering and Management*. 2015;22(1):1-16.10.3846/13923730.2015.1111934
10. Fischer E, Detommaso M, Martinico F, Nocera F, Costanzo V. A risk index for assessing heat stress mitigation strategies. An application in the Mediterranean context. *Journal of Cleaner Production*. 2022;346:131210.10.1016/j.jclepro.2022.131210
11. Khadour N, Fekete A, Sárospataki M. The Role of the Master Plan in City Development, Latakia Master Plan in an International Context. *Land*. 2023;12(8):1634.10.3390/land12081634
12. Khan Z, Javed A. Correlation between land surface temperature (LST) and normalized difference vegetation index (NDVI) in Wardha Valley Coalfield, Maharashtra, Central India. *Nova Geodesia*. 2022;2(3):53.10.55779/ng2353
13. Ghosh S, Kumar D, Kumari R. Assessing spatiotemporal dynamics of land surface temperature and satellite-derived indices for new town development and suburbanization planning. *Urban Governance*. 2022;2(1):144-156.10.1016/j.ugj.2022.05.001
14. Portela CI, Massi KG, Rodrigues T, Alcântara E. Impact of urban and industrial features on land surface temperature: Evidences from satellite thermal indices. *Sustainable Cities and Society*. 2020;56:102100.10.1016/j.scs.2020.102100
15. Kriegler FJ, Malila WA, Nalepka RF, Richardson W. "Preprocessing Transformations and Their Effect on Multispectral Recognition." In Proceedings of the Sixth International Symposium on Remote Sensing of Environment, 97-131. University of Michigan, Ann Arbor, MI, (1969).
16. Avdan U, Jovanovska G. Algorithm for Automated Mapping of Land Surface Temperature Using LANDSAT 8 Satellite Data. *Journal of Sensors*. 2016;2016:1-8.10.1155/2016/1480307
17. Gandhi GM, Parthiban S, Thummalu N, Christy A. NDVI: Vegetation Change Detection Using Remote Sensing and Gis – A Case Study of Vellore District. *Procedia Computer Science*. 2015;57:1199-1210.10.1016/j.procs.2015.07.415
18. Karmoka S, Hanjagi AD. The Impact of Precipitation Distribution on the Natural and Cultivated Vegetation Cover Changes in the Syrian Coastal Area for the Period 2000-2019. *Geo-Eye*. 2022;11(1):6-11.10.53989/bu.ge.v11i1.3
19. Aik DHJ, Ismail MH, Muharam FM. Land Use/Land Cover Changes and the Relationship with Land Surface Temperature Using Landsat and MODIS Imageries in Cameron Highlands, Malaysia. *Land*. 2020;9(10):372.10.3390/land9100372
20. Karmoka ROSA, Jiroudieh A, AL-Jbawi Z. Estimating Age and Tree Density for Jobet Berghal Pinus brutia Ten. Forest Stands Using Landsat ETM Images. 2020;:177-191.10.13140/RG.2.2.26507.50722
21. El-Hattab M, Amany SM, Lamia GE. Monitoring and assessment of urban heat islands over the Southern region of Cairo Governorate, Egypt. *The Egyptian Journal of Remote Sensing and Space Science*. 2018;21(3):311-323.10.1016/j.ejrs.2017.08.008
22. Abdo H, Salloum J. Spatial assessment of soil erosion in Alqerdaha basin (Syria). *Modeling Earth Systems and Environment*. 2017;3(1).10.1007/s40808-017-0294-z
23. Mathbout S, Martin-Vide J, Bustins JAL. Drought characteristics projections based on CMIP6 climate change scenarios in Syria. *Journal of Hydrology: Regional Studies*. 2023;50:101581.10.1016/j.ejrh.2023.101581
24. Alsafadi N, Ansari A, Mokhtar A, Mohammed S, Elbeltagi A, Sammen SS, *et al*. An evapotranspiration deficit-based drought index to detect variability of terrestrial carbon productivity in the Middle East. *Environmental Research Letters*. 2022;17(1):014051.10.1088/1748-9326/ac4765
25. Karmoka SF, Al Haj Ahmad A, Alkhaled EA. Identifying Drought Classes in Northwest Syria Using MODIS Satellite Image Spectral Indices EVI, LAI, TVI. *Scientific Journal of King Faisal University*. 2019;20(1):27–39.10.13140/RG.2.2.20054.37447/1
26. Younes A, Ahmad A, Hanjagi AD, Nair AM. Understanding Dynamics of Land Use & Land Cover Change Using GIS & Change Detection Techniques in Tartous, Syria. *European Journal of Geography*. 2023;14(3):20-41.10.48088/ejg.a.you.14.3.020.041
27. Parveen S, Basheer J, Praveen B. A Literature Review on Land Use Land Cover Changes. *International Journal of Advanced Research*. 2018;6(7):1-6.10.21474/ijar01/7327
28. Mohamed MA. An Assessment of Forest Cover Change and Its Driving Forces in the Syrian Coastal Region during a Period of Conflict, 2010 to 2020. *Land*. 2021;10(2):1-25.10.3390/land10020191
29. Rahmoun T, Zhao W, Hammad M, Hassan M. Ruralization vs. Urbanization Sprawl as Guiding Regional Planning: Development Scenario for Rivers Watershed in the Southern Syrian Coastal Region. *IOP Conference Series: Earth and Environmental Science*. 2018;151:012033.10.1088/1755-1315/151/1/012033
30. Rudel TK, Coomes OT, Moran E, Achard F, Angelsen A, Xu J, *et al*. Forest transitions: towards a global understanding of land use change. *Global Environmental Change*. 2005;15(1):23-31.10.1016/j.gloenvcha.2004.11.001
31. Dudley JP, Ginsberg JR, Plumptre AJ, Hart JA, Campos LC. Effects of War and Civil Strife on Wildlife and Wildlife Habitats. *Conservation Biology*. 2002;16(2):319-329.10.1046/j.1523-1739.2002.00306.x
32. Murphy P, Lobdell D. U.S. Environmental Protection Agency's (EPA) 2008 Report on the Environment (ROE): Identified Gaps and Future Challenges for Human Exposure and Health Indicators. *Epidemiology*. 2009;20:S91.10.1097/01.ede.0000362984.98566.ed
33. Bowler DE, Buyung-Ali L, Knight TM, Pullin AS. Urban greening to cool towns and cities: A systematic review of the empirical evidence. *Landscape and Urban Planning*. 2010;97(3):147-155.10.1016/j.landurbplan.2010.05.006
34. Eum JH, Scherer D, Fehrenbach U, Köppel J, Woo JH. Integrating urban climate into urban master plans using spatially distributed information —The Seoul example. *Land Use Policy*. 2013;34:223-232.10.1016/j.landusepol.2013.03.016